Pergamon

Chemical Engineering Science, Vol. 53, No. 15, pp. 2769–2790, 1998

Printed in Great Britain

PII: S0009–2509(98)00095–5

0009–2509/98/$–See front matter

Experimental studies on optimal molecular weight distribution control in a batch-free radical polymerization process

Timothy J. Crowley and Kyu Yong Choi*

Department of Chemical Engineering, University of Maryland, College Park, MD 20742, U.S.A.

(Received 16 May 1997; accepted 12 February 1998)

Abstract—An experimental study on the control of polymer weight chain length distribution is presented for batch-free radical solution polymerization of methyl methacrylate. The weight chain length distribution is calculated using *the method of finite molecular weight moments* in which the weight fraction of polymers over a number of finite chain length intervals covering the theoretically infinite chain length domain is calculated. Control of a target polymer chain length distribution is achieved by first computing a discrete sequence of reactor temperature setpoints which lead to the best match of a given target weight chain length distribution at a final desired monomer conversion. During the polymerization, an on-line extended Kalman filter is used to incorporate infrequent and delayed off-line molecular weight measurements. The piecewise constant reactor temperature setpoints are taken as the decision variables in a nonlinear programming problem. They are recomputed and updated at each sampling point during the course of polymerization to match the final desired molecular weight distribution. It is demonstrated through simulations and experimentation that it is feasible to control the entire polymer chain length distribution in a batch polymerization process. © 1998 Elsevier Science Ltd. All rights reserved.

Keywords: Molecular weight distribution; free radical polymerization; polymerization reactor control; optimization.

1. INTRODUCTION

The molecular weight distribution (MWD) of a polymer is one of the most important quality control variables in industrial polymerization processes because many of polymer end-use properties are directly dependent on the MWD. However, a direct feedback control of polymer MWD is often a difficult task for several reasons. The primary difficulty arises due to measurement time delays inherent in the measurement of molecular weight averages and MWD. Even with an on-line gel permeation chromatographic system, measurement delays are often on the order of 1 h. For a batch process where reaction time may be short, it will be difficult to utilize only a few delayed measurements and to adjust reaction conditions to attain the target molecular weight or MWD. The problem of measurement delays has been studied by several researchers in recent years using, for example, on-line state estimation techniques such as extended Kalman filtering (EKF) with a process model (Schuler and Suzhen, 1985; Ray, 1986; Ellis *et al*., 1988; Adebekun and Schork, 1989; Kim and Choi, 1991). Kalman filtering introduces its own set of issues including the need to handle data from sensors which are available at different rates and the choice of values for the filter's statistical parameters.

To control polymer MWD it is necessary to select suitable manipulated variables and a control algorithm for on-line applications. In batch processes, manipulated variables must be adjusted to achieve the target molecular weight distribution at the end of the batch. A common method for controlling MWD in batch polymerization reactors is to predetermine the desired control variable trajectories (e.g. temperature set point program or initiator addition policy) by some means (*task level control design*) and then attempt to execute these trajectories during operation (*execution level control*). There has been a great deal of work focused on synthesis of optimal control trajectories for polymerization reactors using Pontryagin's minimum principle. The necessary conditions for an optimal control trajectory, derived from variational calculus and the minimum principle,

* Corresponding author. Tel.: 301 405 1907; fax: 301 314 9126; e-mail: choi@eng.umd.edu.

have been used in many polymerization processes for optimal control synthesis (Hicks and Ray, 1971; Sacks *et al*., 1973; Tirrell and Gromley, 1981; Thomas and Kiparissides, 1984; Ponnuswamy *et al*., 1987). Policies which attempt to maintain constant instantaneous properties are referred to as disjoint policies and can often be derived directly from modeling equations (Hoffman *et al*., 1964; Beste and Hall, 1966; Kozub and MacGregor, 1992; Maschio *et al*., 1994). Other approximate methods of optimal control trajectory synthesis include control vector parameterization (Hicks and Ray, 1971; Choi and Butala, 1991) and nonlinear programming (Tabak and Kuo, 1969; Cuthrell and Biegler, 1988). Many of these optimal control synthesis methods were also tested in laboratory reactors with often very good results. However, problems associated with control based on optimal control trajectories arise in industrial-scale reactors due to process disturbances and modeling errors which can lead to poor control of the MWD. Therefore, in some processes, it may be beneficial to utilize measurements of MWD during a batch process for feedback control to compensate for process disturbances and for trajectories calculated using erroneous models.

Published work considering optimal feedback control of polymer MWD is sparse. This can be attributed to the lack of rapid on-line polymer property sensors. Kozub and MacGregor (1992) developed a method for feedback optimal control of copolymer composition and molecular weight averages for semibatch copolymerization reactors. Their control scheme featured a nonlinear state estimator to infer copolymer properties from on-line measurements and on-line calculation of the disjoint optimal monomer feed rate policies based on the reaction conditions required to maintain constant instantaneous polymer properties. Feedback control was achieved by making corrections to the optimal policies proportional to the deviations of estimated instantaneous polymer properties from their target values. This strategy was tested on a simulated styrene-butadiene emulsion polymerization reactor. However, few experimental studies have been reported on molecular weight distribution feedback control.

The extended Kalman filtering technique was used to estimate and control polymer molecular weight averages in a continuous-stirred-tank styrene polymerization reactor (Kim and Choi, 1991). It was shown that the quality of process model and the frequency of time delayed molecular weight measurements are closely related. They showed through numerical simulations that process transition time can also be reduced if on-line property estimation is available.

Recently, Ogunnaike (1994) developed a two-tier model-based control strategy for a continuous terpolymerization reactor. In the primary tier, flow rates of catalyst, monomers, solvent and chain transfer were manipulated to regulate reactant concentrations in the reactor. A secondary control tier was used to reset the reactant concentration setpoints to control production rate, terpolymer composition, and a melt viscosity indicator variable which was empirically correlated to weight average molecular weight. An extended Kalman filter was used to estimate the terpolymers molecular weight distribution and melt viscosity index on-line based on laboratory melt viscosity measurements. They reported significant reduction in product variability due to this control strategy.

Ellis *et al*. (1994) developed and implemented an on-line estimator for estimation and control of molecular weight distribution in an laboratory reactor for methyl methacrylate solution polymerization. The estimator was based on the extended Kalman filter, incorporating a detailed process model and on-line monomer conversion measurements, temperature measurements, and periodic, time delayed MWD measurements from an on-line size exclusion chromatograph. Because of the measurement delay associated with MWD measurements, a two-time scale extended Kalman filter was used to incorporate fast monomer conversion and temperature measurements as well as delayed molecular weight (chain length) measurements. In their experiments, weight-average molecular weight was controlled using PID controllers. Temperature, monomer-addition rate, and simultaneous temperature and monomer addition rate control were experimentally investigated to achieve a constant weight-average molecular weight during batch polymerization. They concluded that on-line feedback control of molecular weight is feasible and effective in rejecting realistic disturbances which causes the performance of open-loop control strategies to deteriorate.

The control strategy to be presented in this work has been developed with several observations from past work. First of all, most of the reported works were focused on the control of molecular weight averages and polydispersity. However, it may be desirable to control the polymer chain length distribution, not just molecular weight averages (M_n and M_w) for some applications because molecular weight averages may not uniquely characterize a given polymer molecular weight distribution (Ray, 1972). It is not uncommon that two polymers having different chain length distributions may be represented by identical number and weight average molecular weights. Thus, it may be necessary to model and control the entire molecular weight distribution. Little has been published on the direct control of polymer chain length distribution during polymerization. A second observation is that although control of molecular weight by synthesizing and executing optimal control policies has been effectively demonstrated and verified in experimental reactors by many workers, simulation or experimental results may not always automatically translate to industrial scale reactors. It is well known that poor heat transfer and mixing in industrial-scale reactors can affect the accuracy of polymerization models (and optimal trajectories based on these models) which are generally developed with the assumption of perfect mixing. In particular, spatial variations of

temperature within a reactor can have a significant effect on polymer properties. A final observation is derived from the work of Sacks *et al*. (1973). Using the maximum principle, they found that for batch-free radical polymerizations, reactor temperature policies that maximize polydispersity or broaden the MWD will consist of one or at most two step changes in reactor temperature between the upper and lower temperature bounds. Therefore, discrete (rather than continuous) temperature policies may be sufficient in some cases for controlling broad molecular weight distributions.

Based on these observations, in this work we focus on controlling a batch laboratory polymerization reactor to produce a specific target MWD at the end of the batch with final monomer conversion specified. For the design of MWD control system, a deterministic process model must be available. Then a sequence of discrete, piecewise constant reactor temperature set points is developed such that a target MWD is achieved at the final monomer conversion. These temperatures are the decision variables in a nonlinear programming problem with upper and lower bounds on the allowable reactor temperature. Since it is generally expected that some model-plant mismatch may be present, it is necessary to update the initial design of reactor control policies. To make any necessary control adjustment for MWD control, a decoupled extended Kalman filter (EKF) is used to estimate process states observable from on-line measurements (e.g. temperature and conversion) and MWD available from infrequent, delayed measurements. Based on the measured model-plant mismatch in process and polymer quality parameters, corrective control actions are made by solving the nonlinear program with updated state estimates at each sampling point. Although reactor temperature is actually a state variable rather than a free variable, we have chosen to treat reactor temperature as a decision variable with the assumption that reactor temperature can be tracked reasonably well by an execution level controller. The practical reason for this choice is that from an operational standpoint, it is much easier to monitor controller performance by observing a computed sequence of reactor temperature setpoints than by observing optimal values for true manipulated variables such as coolant flow rate, coolant temperature, valve positions, etc. The suboptimal reactor temperature policy is tracked by calculating a sequence of coolant temperatures which again are decision variables in a second nonlinear program with upper and lower bounds on the coolant temperature. It should be noted that if the reactor temperature control itself is the major control problem due to reaction exothermicity, the method proposed in this work may not be directly applicable. In such a case, other control variable may have to be chosen (e.g. initiator addition rate, chain transfer agent addition rate).

2. EXPERIMENTAL SYSTEM

Methyl methacrylate (MMA) was polymerized in a 4 liter stainless steel jacketed reactor with 2,2′-azobis(2-methyl-butanenitrile) (Vazo 67, Dupont) initiator and ethyl acetate solvent. Figure 1 is a schematic diagram of the laboratory batch reactor system. The monomer conversion was determined on-line using a densitometer (DMS/D6, Micromotion). Reactor temperature was controlled by adjusting the setpoint for coolant temperature fed to the reactor's cooling jacket. The coolant temperature was controlled by

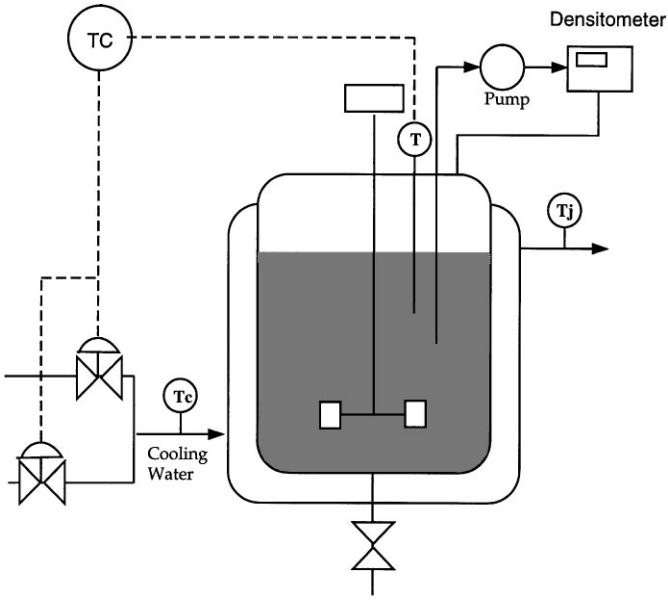

Fig. 1. Schematic of laboratory batch polymerization reactor.

adjusting the flow rates of a hot-water stream and a cold-water stream using two control valves which were interfaced to a microcomputer. Both hot- and cold-water streams were mixed before entering the cooling jacket. The microcomputer acquired temperature and density measurements, updated state estimates, recomputed the suboptimal reactor temperature policy, and calculated control actions for the hot- and cold-water stream valves at 1 min intervals.

A small amount of the reaction mixture was continuously circulated by a gear pump through a sampling loop containing the densitometer and a valve for removal of samples for off-line analysis. Density measurements obtained from the on-line densitometer were used to determine monomer conversion, x_c, according to the relationship

$$x_c = \frac{1/\rho_d - (1/\rho_{d0})}{x_{m0}(1/\rho_p - (1/\rho_m))}. \quad (1)$$

Here, ρ_d represents reaction mixture density as measured by the densitometer, ρ_{d0} the initial density measurement, x_{m0} the initial monomer weight fraction, and ρ_p and ρ_m represent densities of polymer and monomer, respectively. Figure 2 shows that on-line densitometer measurements for a typical batch polymerization experiment agree reasonably well with off-line gravimetric conversion measurements. Off-line conversion measurements were made by weighing a small amount of sample taken from a sampling valve during polymerization, precipitating with excess methanol, drying, and weighing the resulting dry polymer.

Off-line molecular weight measurements were made with a Waters GPC system equipped with a refractive index (RI) detector and three Ultrastyragel columns (one 10^4 Å, one 10^3 Å, and a linear column). Narrow MWD poly(methyl methacrylate) standards were used for column calibration. Polymer samples taken from the reactor at various times during polymerization were precipitated, dried, dissolved in tetrahydrofuran (THF), filtered, and injected into the GPC system. Because the GPC system used in our experimental study was not equipped for on-line sampling and analysis, real feedback control of molecular weight distribution was not possible. Instead, an initial polymerization experiment was used to obtain molecular weight measurements and then a second experiment was conducted under similar reaction conditions with molecular weight measurements from the previous experiment used to update molecular weight predictions and control actions in the second experiment. This procedure will be described in more detail. If an on-line GPC is available in industrial polymerization process systems, the measured GPC data can be directly used to update optimal reactor control program during batch operation.

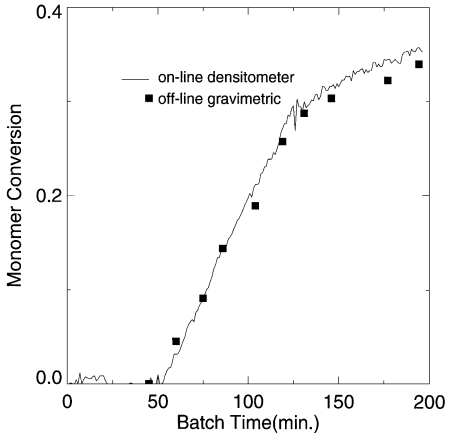

Fig. 2. Comparison of gravimetric and densitometer measured conversion.

3. FREE-RADIAL POLYMERIZATION MODEL

The kinetics of free radical solution polymerization of MMA is relatively well known. The kinetic scheme for MMA polymerization is shown in Table 1 and model parameters used in this study are given in Tables 2 and 3. The gel effect at high monomer conversion is modeled using the correlation proposed by Ross and Laurence (1976):

To provide a smooth function for optimization, the two gel effect correlations are combined in this work as

$$g_t = \begin{cases} g_{t1} = 0.10575\ \exp[17.15v_f - 0.01715(T - 273.16)] & \text{if } v_f \geqslant v_{f\text{cr}} \\ g_{t2} = 2.3 \times 10^{-6}\exp(75v_f) & \text{if } v_f \leqslant v_{f\text{cr}}. \end{cases} \quad (2)$$

$$g_t = 0.5((g_{t1} - g_{t2}) \times \tanh(150(v_f - v_{fcr})) + g_{t1} + g_{t2}). \quad (3)$$

Here, $g_t \equiv k_t/k_{t0}$ (k_{t0} = termination constant at zero monomer conversion), v_f represents free volume and v_{fcr} the critical free volume. They are given by (Schmidt and Ray, 1981):

$$v_f = 0.025 + 0.001(T - 167)\phi_m + 0.001(T - 181)\phi_s + 0.00048(T - 387)\phi_p \quad (4)$$

$$v_{f\text{cr}} = 0.152$$

where ϕ_m, ϕ_s, and ϕ_p represent the volume fractions of monomer, solvent and polymer, respectively, and are given by:

$$\phi_s = \frac{x_s M_t}{\rho_s V}$$

$$\phi_p = \frac{x_p M_t}{\rho_p V} \quad (5)$$

$$\phi_m = 1 - \phi_s - \phi_p$$

Table 1. Kinetic scheme for free-radical polymerization of MMA

Initiation:	$I \xrightarrow{k_d} 2R$
	$R + M \xrightarrow{k_i} P_1$
Propagation:	$P_n + M \xrightarrow{k_p} P_{n+1}$
Chain transfer to monomer and solvent:	$P_n + M \xrightarrow{k_{fm}} D_n + P_1$
	$P_n + S \xrightarrow{k_{fs}} D_n + P_1$
Termination(disproportionation only):	$P_n + P_m \xrightarrow{k_{td}} D_n + D_m$

Table 2. Reactor parameters

Reactor volume(L)	4.0
Jacket volume(L)	3.5
Heat Xfer area(cm^2)	530.0
Coolant flow(L/min)	1.0
Initiator conc.(Mol/L)	0.046
Initial solvent vol. frac.	0.5
Initial monomer vol. frac.	0.5

where x_j represents mass fraction of component j, M_t the total mass, and ρ_j is the density of component j. The total reactor volume, V, is assumed to be an ideal mixture of its components and is given by

$$V = \left(\frac{x_m}{\rho_m} + \frac{x_p}{\rho_p} + \frac{x_s}{\rho_s} + \frac{x_i}{\rho_i}\right) M_t. \tag{6}$$

The modeling equations for a batch MMA polymerization reactor and cooling jacket consist of the following mass and energy balances:

$$\frac{dx_I}{dt} = -k_d x_I \tag{7}$$

$$\frac{dx_p}{dt} = k_p x_m (2-\alpha) P \tag{8}$$

$$\frac{dx_s}{dt} = -k_{fs} x_s P \tag{9}$$

$$\frac{dx_T}{dt} = \frac{(-\Delta H) k_p x_m M_t P}{T_{ref} c_p M_t} - \frac{u_{eff}}{c_p M_t}(x_T - x_J) + x_d \tag{10}$$

$$\frac{dx_J}{dt} = \frac{\rho_c c_{pc} q_c}{\rho_c c_{pc} V_J}(u_c - x_J) + \frac{u_{eff}}{\rho_c c_{pc} V_J}(x_T - x_J) \tag{11}$$

$$x_m = 1 - x_p - x_s - x_I \tag{12}$$

Here, α, the probability of propagation, is defined by

$$\alpha \equiv \frac{k_p M}{k_p M + k_{fm} M + k_{fs} S + k_{td} P}. \tag{13}$$

x_T, x_J and u_c are dimensionless reactor, jacket and coolant temperatures, respectively, defined by

$$x_T \equiv \frac{T}{T_{ref}}$$

$$x_J \equiv \frac{T_J}{T_{ref}}$$

$$u_c \equiv \frac{T_c}{T_{ref}}$$

Table 3. Kinetic parameters for polymerization model (cal,mol,L,K,min)

Experiment I	Ref.	Experiments II and III	Ref.
$k_d = 1.13 \times 10^{19} \exp\left(\frac{-34,277}{RT}\right)$	9	$k_d = 1.13 \times 10^{19} \exp\left(\frac{-34,277}{RT}\right)$	9
$k_p = 4.20 \times 10^{8} \exp\left(\frac{-6,300}{RT}\right)$	24	$k_p = 4.20 \times 10^{8} \exp\left(\frac{-6,300}{RT}\right)$	24
$k_{fm} = 1.50 \times 10^{13} \exp\left(\frac{-17,957}{RT}\right)$	–	$k_{fm} = 3.50 \times 10^{16} \exp\left(\frac{-23,031}{RT}\right)$	–
$k_{fs} = 2.58 \times 10^{11} \exp\left(\frac{-15,702}{RT}\right)$	–	$k_{fs} = 6.95 \times 10^{10} \exp\left(\frac{-15,702}{RT}\right)$	10
$k_{td0} = 1.06 \times 10^{11} \exp\left(\frac{-2,800}{RT}\right)$	24	$k_{td0} = 1.06 \times 10^{11} \exp\left(\frac{-2,800}{RT}\right)$	24
$f_i = 0.1996$	–	$f_i = 0.2055$	–

and T_{ref} is a reference temperature and was set at 373.15 K. u_{eff} is the effective reactor wall heat transfer coefficient. It is assumed that the coolant is perfectly back mixed in the cooling jacket and that the dynamics of the reactor wall are sufficiently fast relative to the dominating process time constants to be neglected. Also, the reaction mixture in the reactor is assumed to be perfectly mixed.

The total concentration of live polymers (P) is derived by applying the quasi-steady-state approximation to live radical species which yields

$$P = \left(\frac{2f_i k_d I}{k_{td}}\right)^{1/2} \tag{14}$$

where f_i is the initiator efficiency factor. The kinetic rate equation for dead polymer of chain length n (D_n) can be derived from the kinetic scheme

$$\frac{\mathrm{d}[D_n V]}{\mathrm{d}t} = V[k_{td}P + k_{fm}M + k_{fs}S]P_n \tag{15}$$

Here, molar concentration of monomer and likewise solvent concentration is related to the corresponding mass fraction as

$$M = \frac{x_m M_t}{w_m V}$$

where w_m is the monomer molecular weight. It is easy to derive the following equation for live polymer concentration:

$$P_n = \alpha P_{n-1} = (1-\alpha)\alpha^{n-1}P. \tag{16}$$

Since our primary objective is to control polymer weight chain length distribution (WCLD), we need a method to compute the polymer WCLD. The reason why we choose WCLD for MWD control is because most of the rheological and mechanical properties of polymer are dependent more strongly on WCLD than on number chain length distribution (NCLD). GPC chromatograms also represent polymer's WCLD because GPC detectors are mostly mass-sensitive detectors. To calculate polymer chain length distribution, eq. (15) could be integrated numerically along with other kinetic equations for n values from 2 to ∞ (or very large value). Obviously, it will be computationally demanding because a very large number of differential and algebraic equations must be solved. However, in this work, we choose to model the weight fraction of polymer in a chain length interval rather than at a specific single chain length. As will be presented later in this paper, the weight fractions of polymers in finite chain length intervals are subject to control. In the following, we outline the method of finite molecular weight moments (Crowley and Choi, 1997a) to perform such calculations.

The weight fractions of polymers in finite chain length intervals can be directly calculated together with other kinetic or reactor modeling equations using the following function that defines the weight fraction of polymer within the chain length interval (m, n):

$$f(m,n) \equiv \frac{\sum_{i=m}^{n} iD_i V}{\sum_{i=2}^{\infty} iD_i V}. \tag{17}$$

Here, we ignore the contribution of live polymers because their concentrations are far smaller than those of dead polymers. If the contribution of live polymers is significant, the live polymer concentration can be easily included in the above formulation. A function that defines the number fraction of polymer within the chain length interval (m, n) can also be defined similarly [i.e. $g(m,n) \equiv \sum_{i=m}^{n} D_i V / \sum_{i=2}^{\infty} D_i V$]. Then we can derive the following equation:

$$\begin{aligned}\frac{\mathrm{d}f(m,n)}{\mathrm{d}t} &= \frac{1}{\lambda_1}\sum_{i=m}^{n} i\frac{\mathrm{d}[D_i V]}{\mathrm{d}t} - \frac{\sum_{i=m}^{n}[iD_i V]}{\lambda_1^2}\frac{\mathrm{d}\lambda_1}{\mathrm{d}t} \\ &= \frac{1}{\lambda_1}\sum_{i=m}^{n} i\frac{\mathrm{d}[D_i V]}{\mathrm{d}t} - \frac{f(m,n)}{\lambda_1}\frac{\mathrm{d}\lambda_1}{\mathrm{d}t}.\end{aligned} \tag{18}$$

Here, $\lambda_1 (\equiv \sum_{n=2}^{\infty}[nD_n V])$ represents the first moment of the molecular weight distribution. Since the weight fractions for certain chain length intervals are calculated and only a small number of chain length intervals can be chosen to represent the polymer chain length distribution, the number of differential equations to solve is reduced dramatically. Another reasons for this choice include the fact that $f(2, \infty)$ should always be equal to 1.0 and therefore this provides an inherent check of the modeling equations. Also, modeling the WCLD in this fashion makes it possible to group polymers with different chain lengths into molecular weight regions in applications where this is useful. For instance, a recent study of the effect of molecular weight distribution on the tensile strength of amorphous polystyrene suggests that all polystyrene molecules with chain lengths less than a threshold chain length do not contribute to the polymer's overall tensile strength and therefore, should be distinguished from polymer's molecules larger than the threshold when developing empirical correlations of tensile strength with MWD (Bersted and Anderson, 1990).

Using eq. (15) and the definition for α, we obtain

$$\sum_{i=m}^{n} i\frac{\mathrm{d}[D_i V]}{\mathrm{d}t} = \frac{k_p M V(1-\alpha)}{\alpha}\sum_{i=m}^{n} iP_i. \tag{19}$$

The term, $\sum_{i=m}^{n} iP_i$, is evaluated as follows:

$$\sum_{i=m}^{n} iP_i = \sum_{i=m}^{\infty} iP_i - \sum_{i=n+1}^{\infty} iP_i \tag{20}$$

where these summations are evaluated by making use of the relationship, $P_n = \alpha P_{n-1}$:

$$\sum_{i=m}^{\infty} iP_i = \left[\frac{m(1-\alpha)+\alpha}{(1-\alpha)^2}\right]P_m. \tag{21}$$

Using this result and the relationship $P_n = (1-\alpha)\alpha^{n-1}P$ we obtain

$$\sum_{i=m}^{n} iP_i = \left[\frac{m(1-\alpha)+\alpha}{(1-\alpha)}\right]\alpha^{m-1}P - \left[\frac{(n+1)\ (1-\alpha)+\alpha}{(1-\alpha)}\right]\alpha^n P. \tag{22}$$

Finally, eq. (18) becomes

$$\frac{df(m,n)}{dt} = \frac{k_p MV}{\lambda_1}\left(\left[\frac{m(1-\alpha)+\alpha}{\alpha}\right]\alpha^{m-1} - \left[\frac{(n+1)(1-\alpha)+\alpha}{(1-\alpha)}\right]\alpha^n\right)P - \frac{f(m,n)}{\lambda_1}\frac{d\lambda_1}{dt}. \tag{23}$$

The kth molecular weight moment, λ_k, is defined as

$$\lambda_k \equiv \sum_{n=2}^{\infty} n^k D_n V.$$

Then, the following molecular weight moment equations are also solved to calculate the molecular weight averages:

$$\frac{d\lambda_0}{dt} = k_p MV(1-\alpha)P \tag{24}$$

$$\frac{d\lambda_1}{dt} = k_p MV(2-\alpha)P \tag{25}$$

$$\frac{d\lambda_2}{dt} = \frac{k_p MV(\alpha^2 - 3\alpha + 4)P}{(1-\alpha)} \tag{26}$$

Weight average and number-average degree of polymerization are calculated by

$$X_n = \frac{\lambda_1}{\lambda_0} \tag{27}$$

$$X_w = \frac{\lambda_2}{\lambda_1}. \tag{28}$$

The method presented above differs from discretizing the polymer population balance equations for numerical calculations in that the equations expressing the weight fraction of polymers in any given chain length interval are explicit and direct. More details of computational procedure can be found in Crowley and Choi (1997a).

4. TASK LEVEL CONTROL OF CHAIN LENGTH DISTRIBUTION

To control the WCLD during batch MMA polymerization,we choose reactor temperature setpoint or setpoint sequence as a task level manipulated variable (or control policy) because polymer chain length is very sensitive to temperature. Of course, this sensitivity is governed by the reaction kinetics and limited by bounds on the allowable reactor temperatures, and it would be possible that a target WCLD chosen may not be physically realizable. However, in our experimental work, we have used target molecular weight distributions which had been previously produced in polymerization experiments.

For complex systems, it is generally infeasible to recompute a continuous optimal control trajectory $u(t)$ on line at each sampling interval because of the considerable computational time required to solve the system and adjoint equations numerically and iteratively find the $u(t)$ which satisfies certain necessary conditions for optimality. Therefore, to approximate an optimal reactor temperature trajectory, we shall determine a sequence of discrete temperature setpoints using nonlinear programming (NLP) technique. The NLP requires a mathematical objective function which adequately describes the real control objective. In the case of a batch homopolymerization, the real control objective in terms of polymer properties might be stated as '*Produce polymer with the desired WCLD at a final monomer conversion of* 40%'. This is an end-point problem with the final time unknown. It is possible that if batch time is also to be minimized, different optimal design of reactor operating policies may be obtained. In our work, however, time optimization problem is not considered.

One difficulty associated with this end-point problem is that the final batch time is unknown. To circumvent this problem, time is replaced by monomer conversion as the independent variable in the model used for optimization. This is accomplished by dividing eqs (7)–(9), and (23) at 15 discrete chain lengths, by the following equation for monomer conversion:

$$\frac{dx_c}{dt} = \frac{(k_p + k_{fm})x_m P}{x_{m0}}. \tag{29}$$

This procedure enables the final value of the independent variable, monomer conversion, to be anchored at its desired final value in all computations.

The dynamic model used for optimization computations becomes

$$\frac{dx_p}{dx_c} = \frac{x_{m0}k_p(2-\alpha)}{k_p + k_{fm}} \tag{30}$$

$$\frac{dx_I}{dx_c} = -\frac{x_{m0}(k_d x_I)}{(k_p + k_{fm})x_m P} \tag{31}$$

$$\frac{dx_s}{dx_c} = -\frac{x_{m0}(k_{fs}x_s)}{(k_p + k_{fm})x_m} \tag{32}$$

$$\frac{df(m,n)}{dx_c} = \frac{x_{m0}k_p MV\left(\left[\frac{m(1-\alpha)+\alpha}{\alpha}\right]\alpha^{m-1} - \left[\frac{(n+1)(1-\alpha)+\alpha}{\alpha}\right]\alpha^n\right)}{(k_p + k_{fm})x_m\lambda_1} - \frac{x_{m0}}{(k_p + k_{fm})x_m P}\frac{f(m,n)}{\lambda_1}\frac{d\lambda_1}{dt}. \tag{33}$$

The objective function can then be defined in terms of the final batch WCLD alone:

$$J(\mathbf{u}, x_{cf}) = \sum_{i=1}^{15}(f(2 + a(i-1)i, 1 + ai(i+1)) - f_{i,\text{set}})^2 \tag{34}$$

where $\mathbf{u}$ is a vector representing the sequence of reactor temperature setpoints during the batch which are calculated using a sequential quadratic programming algorithm (Crowley and Choi, 1997b), x_{cf} is the fixed desired final monomer conversion and $f_{i,\text{set}}$ the desired WCLD values. Notice that in the above the polymer

chain length distribution has been divided into 15 discrete intervals. The reactor temperature setpoints are discretized in conversion rather than time. Therefore, each element of the vector **u** is a temperature setpoint at which the reactor will be controlled for a fixed fraction of the total polymer to be produced. For example, if the final desired monomer conversion were 40% and if the dimension of **u** is 4, the first element of **u** would represent an optimized temperature setpoint at which the reactor would be operated during polymerization from 0 to 10% monomer conversion. The second element of **u** would represent the optimized temperature for conversion from 10 to 20%, the third during polymerization from 20 to 30% monomer conversion and finally, the fourth element would represent the optimized reactor temperature from 30% to the final desired conversion.

The dimension of **u**, denoted by j, the number of reactor temperature setpoints over which the objective function is minimized at each sampling point, is chosen as a compromise of control precision with computational speed. For this work, j was set equal to 5. It should be noted that time required for reoptimization calculation at each sampling point was small enough for the implementation of a real-time feedback controller on our process control computer with a 1 minute sampling time. The objective function can be expressed more succinctly as

$$\min J_k(u_j(j=1,5), x_{cf}) = \sum_{i=1}^{15} (f(2 + a(i-1)i, 1 + ai(i+1)) - f_{i,\text{set}})^2 \quad (35)$$

subject to bounds on the discrete temperature policies, u_j

$$49^\circ\text{C} \leqslant u_j \leqslant 70^\circ\text{C}$$

where the u_j represent a sequence of reactor temperature setpoints up to the final desired weight fraction and J_k represents the task level objective function at the kth sampling time. This objective function is minimized using FSQP (Feasible Sequential Quadratic Programming) (Panier and Tits, 1993). FSQP solves a given optimization problem by iteratively calculating a feasible search direction which is the solution to a quadratic program and which yields a decrease in the objective function. Other similar optimization techniques may be used.

In this work, the objective function is evaluated by integrating eqs (30)–(33) from the current monomer conversion to the final desired monomer conversion. Figure 3 is a block diagram summary of the control algorithm. Here, the subscript k represents the kth sampling point for a batch reactor operated under digital control and the sampling time was 1 min in actual experiments. $u_{1,k}$ represents output from the task level controller block at the kth sampling time. At each time-step, the entire sequence can be recomputed.

5. EXECUTION LEVEL CONTROL

5.1. *State estimation*

The execution level controller block in Fig. 3 represents control of the reactor temperature by manipulating the temperature of the cooling water fed to the reactor's jacket. As seen in this figure, output from a state estimator is used by the execution level controller as well as the task level controller. State estimation is necessary for several reasons. First of all, the estimator provides estimates of states (conversion, polymer concentrations, temperature, weight fractions of polymers in different chain length intervals) using temperature, conversion, and infrequent and

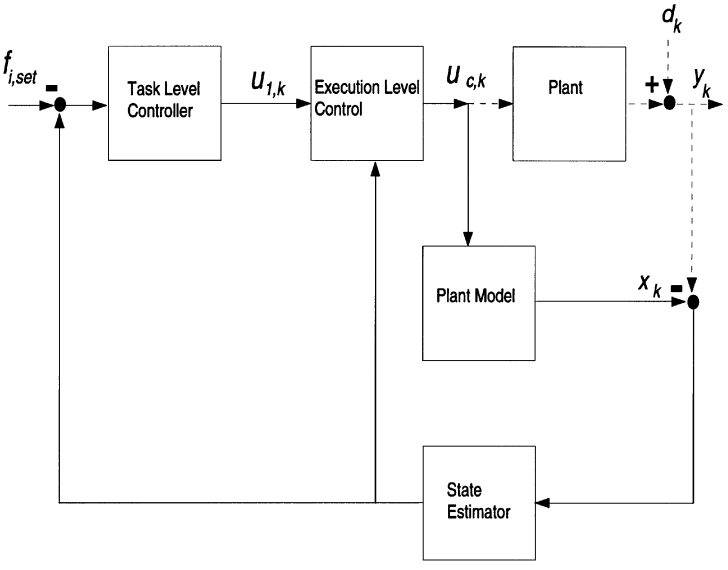

Fig. 3. Block diagram of discrete MWD control.

time-delayed molecular weight measurements which are generally corrupted with stochastic noise. The estimator also provides estimates of unmeasured states such as initiator concentration as well as disturbance states which are required to eliminate plant-model mismatch in model predictive control schemes.

Two decoupled extended Kalman filters (EKF) were developed to estimate reactor state variables observable from on-line measurements, eqs (7)–(11), and those observable from delayed GPC measurements, eqs (23) and (24)–(26). For an analysis of polymer property observability with different combinations of sensors, refer to Ray (1986). Decoupling has the advantage of reducing the number of covariance calculations and simplifying the updating procedure when delayed molecular weight measurements become available. The first filter consists of the set of state variables which are observable from on-line measurements taken at 1 minute intervals. This set of state variables consists of

$$\mathbf{x}_1 = [x_I, x_p, x_T, x_J, x_d] \tag{36}$$

where x_d represents a disturbance state which is estimated to eliminate mismatch between model predicted and measured reactor temperature for the predictive temperature control algorithm described in the next section. The second filter consists of those variables observable from infrequent and delayed WCLD measurements:

$$\mathbf{x}_2 = [\lambda_0, \lambda_1, \lambda_2, f(m, n)] \tag{37}$$

In this work both filters are cast into a continuous-discrete form. The continuous step of the algorithm is the prediction of state and error covariance propagation in the time between discrete measurements. This is achieved by integrating the model and error covariance equations numerically. The discrete step involves updating the predicted state and error covariance estimates when discrete measurements are taken. It should be noted that state propagation is not decoupled since all the states are obviously coupled in some way, but error covariance propagation, and state and error covariance updates are decoupled.

A nonlinear stochastic process model of the state vector, $\mathbf{x}$, and measurement vector, $\mathbf{y}_k$, are expressed as

$$\dot{\mathbf{x}}(t) = \mathbf{f}(\mathbf{x}(t), t) + \mathbf{w}(t), \qquad \mathbf{w}(t) \sim \eta(\mathbf{0}, \mathbf{Q}(t)) \tag{38}$$

$$\mathbf{y}_k = \mathbf{h}_k(\mathbf{x}(t_k)) + \mathbf{v}_k, \quad k = 0, 1, 2 \ldots, \quad \mathbf{v}_k \sim \eta(\mathbf{0}, \mathbf{R}_k). \tag{39}$$

The EKF equations for the state vector estimate, $\hat{x}$, and error covariance matrix, $\mathbf{P}$, are expressed as follows.

state and error covariance prediction:

$$\dot{\hat{\mathbf{x}}}(t) = \mathbf{f}(\hat{\mathbf{x}}(t), t) \tag{40}$$

$$\dot{\mathbf{P}}(t) = \mathbf{F}(\hat{\mathbf{x}}(t), t)\,\mathbf{P}(t) + \mathbf{P}(t)\mathbf{F}^T(\hat{\mathbf{x}}(t), t) + \mathbf{Q}(t) \tag{41}$$

state and error covariance update:

$$\hat{\mathbf{x}}_k(+) = \hat{\mathbf{x}}_k(-) + \mathbf{K}_k[\mathbf{y}_k - \mathbf{h}_k(\hat{\mathbf{x}}_k(-))] \tag{42}$$

$$\mathbf{P}_k(+) = [\mathbf{I} - \mathbf{K}_k(\hat{\mathbf{x}}_k(-))]\mathbf{P}_k(-) \tag{43}$$

where, $\mathbf{K}_k$, the filter gain matrix, is given by

$$\mathbf{K}_k = \mathbf{P}_k(-)\mathbf{H}_k^{\mathrm{T}}(\hat{\mathbf{x}}_k(-))\,[\mathbf{H}_k(\hat{\mathbf{x}}_k(-))\,\mathbf{P}_k(-) \times \mathbf{H}_k^{\mathrm{T}}(\hat{\mathbf{x}}_k(-)) + \mathbf{R}_k]^{-1} \tag{44}$$

and where

$$\mathbf{F}(\hat{\mathbf{x}}(t), t) \equiv \left.\frac{\partial \mathbf{f}(\mathbf{x}(t), t)}{\partial \mathbf{x}(t_k)}\right|_{\mathbf{x}(t) = \hat{\mathbf{x}}(t)} \tag{45}$$

$$\mathbf{H}_k(\hat{\mathbf{x}}_k(-)) \equiv \left.\frac{\partial \mathbf{h}_k(\mathbf{x}(t_k))}{\partial \mathbf{x}(t_k)}\right|_{\mathbf{x}(t_k) = \hat{\mathbf{x}}_k(-)} \tag{46}$$

It is assumed that modeling and measurement errors are independent of each other and therefore, the model and measurement error covariance matrices, **Q** and **R,** are diagonal matrices whose elements are also assumed constant.

Since the polymerization process model is expected to provide a reasonably accurate prediction of actual process behaviors in our reactor system, the unknown disturbance state, x_d, in the first filter is modeled as a random walk variable driven by white noise, $w(t)$:

$$\frac{\mathrm{d}x_d}{\mathrm{d}t} = w(t). \tag{47}$$

Incorporation of delayed molecular weight measurements into the second filter is achieved as follows (Ray, 1986; Ellis *et al*., 1988; Adebekun and Schork, 1989; Kim and Choi, 1991). When the results of a measurement taken at time $t_k - \tau$ become available at t_k (τ = measurement delay time), the old estimates of $\hat{\mathbf{x}}(t_k - \tau)$ and $\mathbf{P}(t_k - \tau)$ are updated using eqs (42)–(43). Then, the trajectories of the state variables are recalculated from $t_k - \tau$ to t_k. This requires computer memory storage of all measurement data acquired between $t_k - \tau$ and t_k and storage of the state estimate values and error covariance matrix values at $t_k - \tau$.

On-line implementation of the EKF requires suitable selection of values for the elements of the measurement error covariance matrix, **R**, and the model error covariance matrix, **Q**. Measurement error covariance values represent the noise or variance of specific sensors and as such can be determined from repetitive experimental measurements. The measurement error covariance matrix for filter 1 has the form

$$\mathbf{R}_{1,k} = \mathrm{diag}[r_{x_p}^2, r_{x_T}^2, r_{x_{Tj}}^2]. \tag{48}$$

Variances of thermocouple measurements and conversion measurements were roughly estimated from experimental observations but variance in WCLD measurements was more difficult to determine. This is because performing a large number of repetitive GPC measurements is extremely time consuming. In this work, several repeated measurements of the same sample were made to obtain an estimate of the

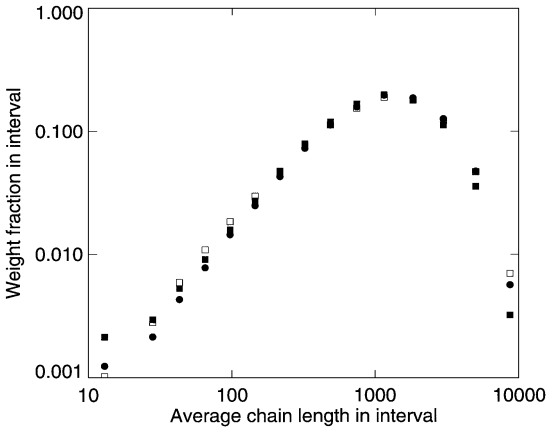

Fig. 4. Three repeated GPC measurements.

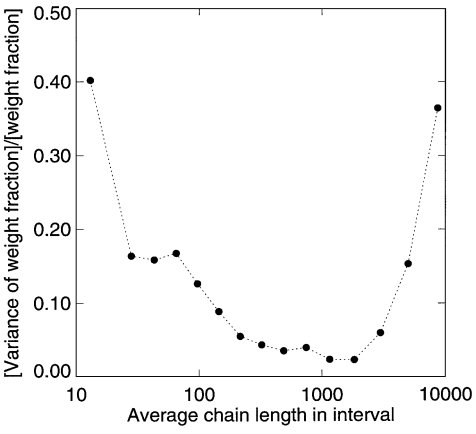

Fig. 5. Variance of MWD weight fractions vs chain length.

WCLD measurement error covariance values. Figure 4 represents three repetitive measurements of WCLD for a polymer sample. This figure shows that molecular weight measurements at the high and low ends of chain length have higher variance than those at intermediate chain lengths given that the signal to noise ratio approaches zero as the signal itself approaches the chromatogram baseline. This behavior can be seen more clearly in Fig. 5 which is a plot of the ratio of variance to weight fraction of polymer in different chain length intervals versus mean chain length in the chain length interval. This figure shows that WCLD measurement error covariances are a function of chain length. The results of this analysis as well as measurement error covariance values for temperature and conversion measurements are given in Table 4. The measurement error covariance matrix for filter 2 has the form:

$$\mathbf{R}_{2,k} = \mathrm{diag}[r^2_{\lambda_{0,\mathrm{set}}}, r^2_{\lambda_{1,\mathrm{set}}}, r^2_{\lambda_{2,\mathrm{set}}}, r^2_{f_{1,\mathrm{set}}}, r^2_{f_{2,\mathrm{set}}}, \cdots, r^2_{f_{n,\mathrm{set}}}]. \quad (49)$$

Values for the diagonal elements of the model error covariance matrix for filter 2, $\mathbf{Q}_2$, are used as tuning parameters since actual model error is rarely known. In this work, reasonable model error covariance values for the molecular weight distribution states were obtained first by assuming the following form for the covariance values.

$$\mathbf{Q}_2(t) = \mathrm{diag}[q^2_{\lambda_{0,\mathrm{set}}}, q^2_{\lambda_{1,\mathrm{set}}}, q^2_{\lambda_{2,\mathrm{set}}}, q^2_{f_{1,\mathrm{set}}}, q^2_{f_{2,\mathrm{set}}}, \cdots, q^2_{f_{n,\mathrm{set}}}]$$

$$q_{f_{i,\mathrm{set}}} = c \times f_{i,\mathrm{set}} \quad (50)$$

where n is the total number of weight fractions of the WCLD to be modeled and controlled which was set at 15 for this work, $f_{i,\mathrm{set}}$ is the ith weight fraction of the target WCLD, and c is a constant to be determined. This form for the covariance matrix elements scales the individual covariance elements to coincide roughly with the scale of the individual WCLD weight fractions since values for the weight fractions at the high and low end of chain length space are relatively smaller than those at intermediate chain lengths. This can be seen in Table 5 which tabulates the target weight fractions used in this work. The constant c was determined by guessing a trial value, simulating off-line the estimation of WCLD for Experiment I, comparing WCLD estimates to actual GPC measurements of WCLD, and reguessing a trial value for c until filter performance was acceptable. Model error covariance values used in this work are given in Table 4.

5.2. *Model-predictive temperature control*

To use reactor temperature setpoints as suboptimal control policies, we have assumed that the

Table 4. Statistical parameters for EKF

EKF 1
$r_{x_P} = 0.005,\ r_{x_T} = 0.000435,\ r_{x_I} = 0.000435$
$q_{x_P} = 0.0014,\ q_{x_T} = 0.03,\ q_{x_{TJ}} = 0.04,\ q_{x_I} = 0.00003$

EKF 2
$r_{f_{1,\mathrm{set}}} = 0.0019,\ r_{f_{2,\mathrm{set}}} = 0.0066, r_{f_{3,\mathrm{set}}} = 0.0072,\ r_{f_{4,\mathrm{set}}} = 0.0043$
$r_{f_{5,\mathrm{set}}} = 0.0047,\ r_{f_{6,\mathrm{set}}} = 0.0064, r_{f_{7,\mathrm{set}}} = 0.0041,\ r_{f_{8,\mathrm{set}}} = 0.0033$
$r_{f_{9,\mathrm{set}}} = 0.0025,\ r_{f_{10,\mathrm{set}}} = 0.0023, r_{f_{11,\mathrm{set}}} = 0.0020, r_{f_{12,\mathrm{set}}} = 0.0015$
$r_{f_{13,\mathrm{set}}} = 0.00081, r_{f_{14,\mathrm{set}}} = 0.00043, r_{f_{15,\mathrm{set}}} = 0.00059$
$r_{\lambda_0} = 0.941 \times 10^{-5}, r_{\lambda_1} = 1.0,\ r_{\lambda_2} = 85.0$
$q_{f_{i,\mathrm{set}}} = 0.05 f_{i\ \mathrm{set}}$
$q_{\lambda_0} = 0.000035,\ q_{\lambda_1} = 0.00141,\ q_{\lambda_2} = 35.0$

temperature setpoints can be tracked closely by a temperature controller. In large-scale industrial reactors, heating and cooling is often difficult due to poor heat transfer and highly exothermic polymerization reactions. In such cases, model-predictive temperature control offers the inherent benefits of accounting for constraints on reactor heat transfer capability (i.e. coolant flow rate or temperature constraints) as well as accounting for the high degree of nonlinearity common in polymerization reactors by computing control actions based on a detailed process model.

Successful implementation of a model predictive controller requires a reasonably accurate model. In developing the energy balance equations [eqs (10) and (11)], perfect mixing of reactor and cooling jacket contents was first assumed. Experiments in our lab-scale reactor have shown that mixing behavior can be quite different from that of perfect mixing in the cooling jacket operated at a relatively large mean residence time. In all experiments, cooling water feed flow rate was fixed at 1 L/min using a ratio controller to adjust the two control valves for hot and cold water respectively. The cooling jacket volume was 3.5 L corresponding to a mean residence time of 3.5 min. Figure 6 represents a test experiment in which two large step changes in coolant feed temperature were made and the corresponding reactor and jacket temperatures were recorded. The reactor contained 1 L of ethyl acetate at an initial temperature of 35°C and the agitator was set to a high speed to ensure vigorous mixing of the reactor contents. This figure shows that jacket effluent temperature begins to rise almost immediately after the coolant temperature is increased. This is consistent with a perfect mixing model for the jacket which predicts that jacket temperature should respond almost instantaneously to an increase in coolant feed temperature. However, when coolant feed temperature is decreased, the reactor temperature initially leads the jacket effluent temperature which is inconsistent with the perfect mixing model. In fact, the jacket temperature remains essentially unchanged for about 2 min after the step decrease in coolant feed temperature. Since the coolant flow rate is fixed at 1 L min^{-1}, the differences in mixing behavior between heating and cooling may be due to differences in natural convection rates. Coolant enters the jacket from its base and exits at its top. When a step increase in coolant temperature is made, the density of water in the jacket is greater than that of the higher temperature coolant entering at its base. Therefore, buoyancy forces the higher–temperature coolant to the top and the lower temperature jacket water to the bottom. However, when a step decrease in coolant temperature is made, the density of coolant entering at the bottom of the jacket is higher than that of the jacket contents and therefore a buoyancy driving force for natural convection does not exist. It is possible that this effect can also be quite significant in large industrial polymerization reactors.

To improve the cooling jacket model, the jacket was divided into two perfectly mixed virtual volumes.

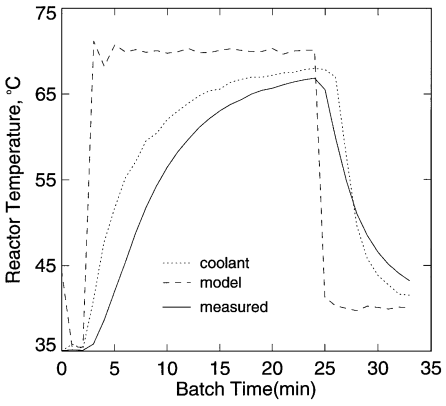

Fig. 6. Temperature step response.

Furthermore, a recycle parameter, denoted q_r, was added to model backmixing of cooling water from the upper jacket volume, v_2, to the lower jacket volume, v_1, when the coolant feed temperature is higher than the jacket effluent temperature. It is assumed that no backmixing occurs when the coolant feed temperature is lower than the jacket temperature. Also, since transmission of coolant in the plumbing from the control valves to the actual jacket inlet requires a finite time, a dead time, τ_d, for coolant temperature changes is included. Finally, loss of heat to the surroundings is considered by adding convective terms to the energy balances. The resulting energy balance model becomes

$$c_p M_t \frac{\mathrm{d}x_T}{\mathrm{d}t} = \frac{(-\Delta H) k_p x_m M_t P}{T_{\mathrm{ref}}} + u_{\mathrm{eff},1}(x_{J1} - x_T) + u_{\mathrm{eff},o}(x_a - x_T) + x_d \tag{51}$$

$$\rho_c c_{pc} v_1 \frac{\mathrm{d}x_{J1}}{\mathrm{d}t} = \rho_c c_{pc} q_c (u_{c,t-\tau_d} - x_{J1}) + u_{\mathrm{eff},1}(x_{\mathrm{T}} - x_{J1}) + u_{eff,a}(x_a - x_{J1}) + \rho_c c_{pc} q_r (x_{J2} - x_{J1}) \tag{52}$$

$$\rho_c c_{pc} v_2 \frac{\mathrm{d}x_{J2}}{\mathrm{d}t} = \rho_c c_{pc} q_c (x_{J1} - x_{J2}) + \rho_c c_{pc} q_r (x_{J1} - x_{J2}) \tag{53}$$

where $u_{\mathrm{eff},1}$ represents the effective heat transfer coefficient between reactor and jacket, $u_{\mathrm{eff},a}$ represents the effective heat transfer coefficient for energy lost from the jacket to the surroundings, and $u_{\mathrm{eff},o}$ represents the effective heat transfer coefficient for energy lost from the reactor to the surroundings. x_a represents the dimensionless ambient temperature, x_{J1} and x_{J2} represent dimensionless temperatures of jacket volumes v_1 and v_2, respectively. Here, $q_r = 0$, for $x_{J1} \leqslant x_{J2}$.

Figure 7 represents the temperature profiles for a polymerization experiment in which two large step changes in reactor temperature were made. The recorded reactor, jacket, and coolant temperature data were used to refine the model parameters in eqs (51)–(53) using FSQP optimization package. The

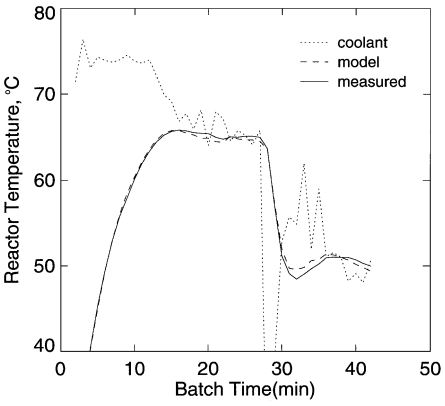

Fig. 7. Comparison of measured and model predicted reactor temperature.

resulting model predictions of reactor temperature with new parameters are compared with measurements in Fig. 7 and values for the optimized model parameters are given in Table 5. Dead time associated with coolant temperature changes was implemented by integrating the modeling equations from time t_{k-1} to $t_{k-1} + \tau_d$ with the coolant temperature fixed at its value measured at t_{k-1} followed by integration from $t_{k-1} + \tau_d$ to t_k with the coolant temperature fixed at its value measured at t_k. Figure 7 shows that with the revised cooling jacket model and parameters, more accurate temperature tracking is obtainable.

The predictive temperature control algorithm used in this work simply involves computing a discrete sequence of coolant temperatures at each sampling point during polymerization, which are the decision variables in a nonlinear programming problem. The NLP finds the sequence which minimizes the objective function

$$\min_{u_{c,k},\ldots,u_{c,k+N-1}} J'_k = \sum_{j=k+1}^{k+p} (u_{1,j} - \hat{x}_{T,j})^2 \qquad (54)$$

subject to bounds on the coolant temperature:

$$35^\circ\text{C} \leqslant u_{c,k} \leqslant 75^\circ\text{C}.$$

Here k represents the current sampling point, J'_k the execution level objective function, $\hat{x}_{T,j}$ the predicted reactor temperature at the jth sampling time in the future, p represents the predicition horizon and N represents the number of future manipulated variable moves. $u_{c,k}$ represents the coolant temperature at the kth sampling point and the predicted reactor temperatures, $\hat{x}_{T,j}$, were computed using eqs (51)–(53).

N and p are tuning parameters. As the number of manipulated variable moves (N) increases, the controller has more freedom in matching output predictions to the setpoint and can produce tighter control but at the expense of larger moves and potential instability. Garcia and Morshedi (1986) report that stability in dynamic matrix control (DMC) is ensured by selecting $p = N + M$ where M is the number of time intervals for a system to reach a steady state. In this work, a value of 4 representing a 4 min prediction horizon was selected for p. N was set at 2, although these may not represent the best values. Therefore, at each sampling point, the execution level controller computes the coolant feed temperature for the current time, t_k and for the next sampling time, t_{k+1} and the future reactor response is predicted out to t_{k+4}.

Because of the dead time associated with coolant temperature changes, the model-based temperature controller is slightly modified to compute the suboptimal sequence of coolant temperatures which best track the desired reactor temperature set point starting at t_{k+2} rather than at the next time interval, t_{k+1}. This has the effect of reducing the magnitude of control actions without penalizing control actions explicitly in the objective function. Equation (54) can then be rewritten with the lower index in the summation changed to $k + 2$:

$$\min_{u_{c,k},u_{c,k+1}} J'_k = \sum_{j=k+2}^{k+4} (u_{1,j} - \hat{x}_{T,j})^2. \qquad (55)$$

Table 5. Optimized parameters for energy balance equations

$u_{\text{eff},1}$	0.817 kcal min^{-1}
c_p	0.4 kcal kg^{-1} K^{-1}
v_1	1.784 L
v_2	2.576 L
$u_{\text{eff},o}$	0.00445 kcal min^{-1}
q_r	19.99 L min^{-1}
τ_d	0.572 min
$u_{\text{eff},a}$	0.0623 kcal min^{-1}

6. RESULTS AND DISCUSSION

Three experiments (experiments I, II and III) have been carried out to illustrate implementation of the overall control strategy in a laboratory batch polymerization reactor. Experiment I illustrates design and execution of a reactor temperature setpoint program to match a prespecified target molecular weight distribution at 40% monomer conversion at the end of batch. Experiment II demonstrates how delayed molecular weight measurements can be incorporated by a state estimator to improve on-line estimates of molecular weight distribution. Finally, Experiment III is used to illustrate how the temperature setpoint program is adjusted on-line as a result of updated molecular weight estimates. Experimental reaction conditions are given in Table 2.

6.1. *Design of temperature setpoint program and execution*

The optimizer FSQP iteratively computes a sequence of reactor temperature set points which will yield the best match between the target and predicted polymer WCLD at the end of the batch corresponding to 40% monomer conversion. The target molecular weight distribution (weight fractions in finite chain length intervals) specified for Experiment I is given in Table 6. The design of a setpoint program

(temperature set point sequence) for this experiment is shown in Fig. 8 which presents snap shots of the computation at three selected iterations starting at zero monomer conversion. Recall that the method of finite molecular weight moments described earlier in this paper has been used in conjunction with the process model and the optimization software (FSQP) to calculate the temperature sequence. Graphs on the left-hand side of this figure represent the computed sequence of reactor temperature setpoints and graphs on the right-hand side represent the resulting predicted WCLD at final monomer conversion of 40%. Figure 8(A1) (labeled 1 Iteration) represents the initialized values for the reactor temperature set point sequence at zero batch time. Here, all values of u_j were initialized at 50°C. The modeling equations were then integrated from 0 to 40% conversion to compute the resulting WCLD which is shown in Fig. 8(B1) along with the target distribution. Since the temperature profile used is not optimal, large discrepancies in the final WCLD result. Figure 8(A2) represents the sequence of reactor temperature setpoints computed by FSQP at the 10th iteration and Fig. 8(B2) shows the resulting WCLD for this sequence. Convergence was achieved at 20 iterations and the suboptimal reactor temperature setpoint sequence is shown in Fig. 8(A3) along with the corresponding comparison of simulated and target WCLD in Fig. 8(B3). In the presence of model-plant mismatch, the implementation of the reactor temperature sequence [e.g. Fig. 8(A3)] may lead to some errors in the final WCLD. Therefore, this temperature set point policy will be updated during the execution control based on the measurements or estimates of polymer MWD.

Remarks: It should be noted that the optimization algorithm, FSQP, may find local rather than global minima. As such, solutions can be sensitive to initial conditions when more than one minimum exists in the solution space. It would often be necessary to properly initialize the optimization procedure when local minima are expected to exist and to evaluate any process constraints (e.g. heat removal capacity) associated with these control designs (Crowley and Choi, 1997b).

For a laboratory polymerization reactor, the feasibility of tracking the temperature setpoint profiles has been tested. Figure 9 presents setpoint program tracking in Experiment I as well as on-line estimates of the disturbance state for the reactor energy balance model. As seen in this figure, maximum deviations of disturbance estimates from zero are on the order of $0.001\ \mathrm{min}^{-1}$ which is equivalent to $0.373\ \mathrm{K\,min}^{-1}$. This figure also shows that rapid and stable setpoint tracking is achieved using the model-predictive controller used in our study, though it should be noted that the small reactor size and relatively large heat transfer capacity are not representative of an industrial-scale reactor in which temperature control can be considerably more difficult. In an industrial polymerization process where more sluggish temperature response is expected, updated reactor temperature setpoint sequence during batch operation may be dependent on the performance of temperature tracking control.

Figure 10(A) presents estimates of weight average (X_w) and number average (X_n) degree of polymerization during the batch and Fig. 10(B) shows a comparison of molecular weight distribution estimates at final conversion to the target distribution. Because the execution level controller tracks the temperature setpoint program well and model-plant mismatch was minimal in the simulation, estimates of the molecular weight distribution at final conversion coincide with the target distribution. However, it is obviously necessary to compare actual molecular weight distribution measurements to the target distribution to evaluate the efficacy of this method. It is also important to compare on-line estimates of monomer conversion to

Table 6. Target WCLD

Experiment I			Expriment II, III		
Chain length interval	Mean	Target weight fraction	Chain length interval	Mean	Target weight fraction
8612–5273	6942	$f_{1,\mathrm{set}} = 0.0021$	15539–8644	12091	$f_{1,\mathrm{set}} = 0.0056$
5272–3331	4301	$f_{2,\mathrm{set}} = 0.0108$	8643–4994	6818	$f_{2,\mathrm{set}} = 0.0471$
3330–2161	2745	$f_{3,\mathrm{set}} = 0.0475$	4993–2983	3988	$f_{3,\mathrm{set}} = 0.1265$
2160–1434	1797	$f_{4,\mathrm{set}} = 0.1246$	2982–1835	2408	$f_{4,\mathrm{set}} = 0.1860$
1433–969	1201	$f_{5,\mathrm{set}} = 0.1893$	1834–1157	1495	$f_{5,\mathrm{set}} = 0.1959$
968–664	816	$f_{6,\mathrm{set}} = 0.1873$	1156–745	950	$f_{6,\mathrm{set}} = 0.1574$
663–459	561	$f_{7,\mathrm{set}} = 0.1556$	744–488	616	$f_{7,\mathrm{set}} = 0.1121$
458–319	388	$f_{8,\mathrm{set}} = 0.1103$	487–323	405	$f_{8,\mathrm{set}} = 0.0722$
318–222	270	$f_{9,\mathrm{set}} = 0.0687$	322–216	269	$f_{9,\mathrm{set}} = 0.0425$
221–153	187	$f_{10,\mathrm{set}} = 0.0427$	215–145	180	$f_{10,\mathrm{set}} = 0.0247$
152–105	128	$f_{11,\mathrm{set}} = 0.0269$	144–97	120	$f_{11,\mathrm{set}} = 0.0143$
104–71	87	$f_{12,\mathrm{set}} = 0.0167$	96–65	80	$f_{12,\mathrm{set}} = 0.0078$
70–47	58	$f_{13,\mathrm{set}} = 0.0092$	64–43	53	$f_{13,\mathrm{set}} = 0.0043$
46–31	38	$f_{14,\mathrm{set}} = 0.0042$	42–28	35	$f_{14,\mathrm{set}} = 0.0021$
30–2	16	$f_{15,\mathrm{set}} = 0.0013$	27–2	14	$f_{15,\mathrm{set}} = 0.0012$

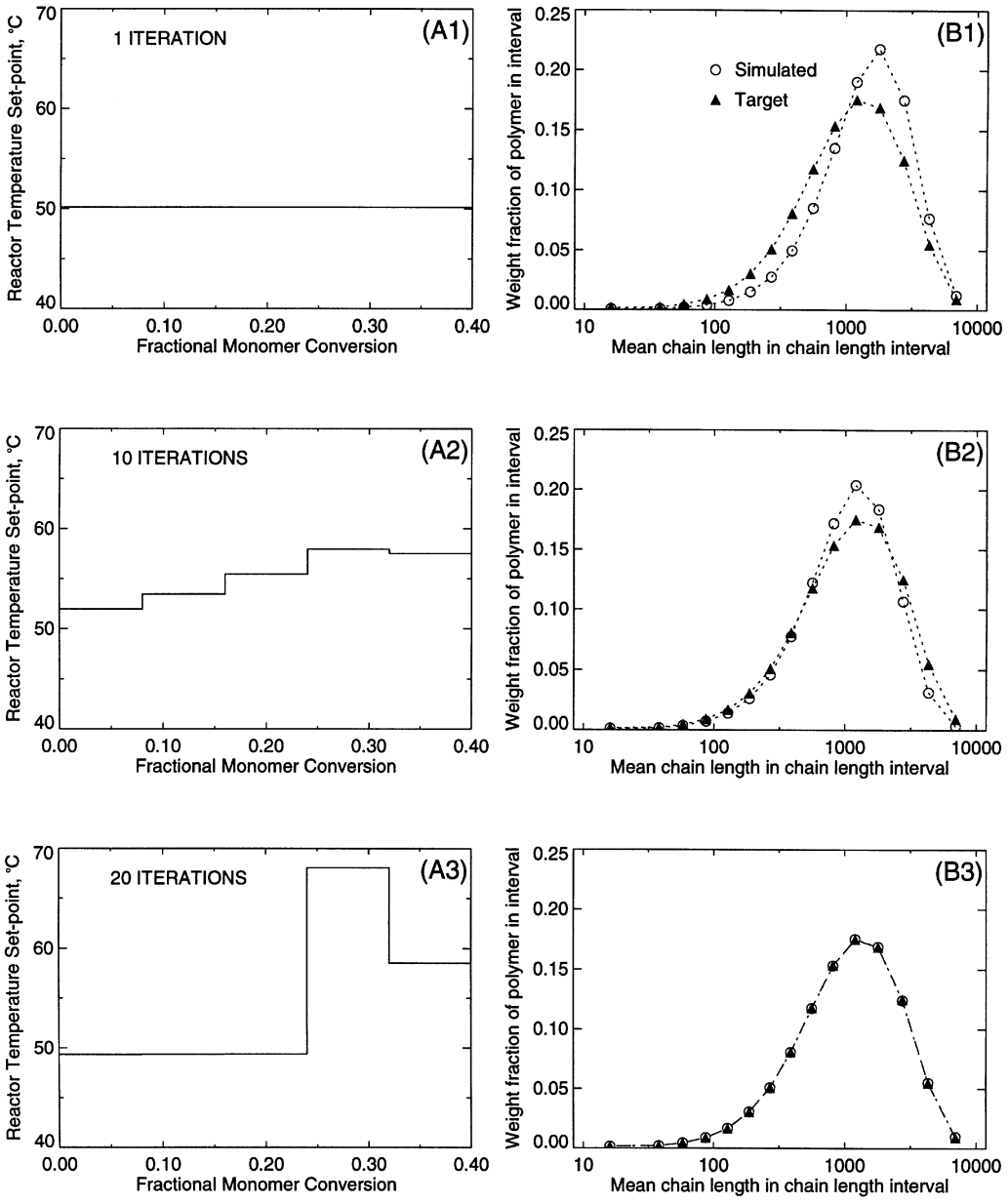

Fig. 8. Design of reactor temperature setpoint program.

off-line conversion measurements since monomer conversion (rather than time) is the reaction coordinate for optimization calculations.

Figure 11 is a comparison of on-line estimates and densitometer measurements of monomer conversion to off-line gravimetric measurements. It should be noted that monomer conversion estimates actually refer to polymer weight fraction (x_p) estimates which are then converted to units of monomer conversion for presentation purposes. This figure shows that density measurements of monomer conversion were slightly higher than gravimetric measurements. This behavior is probably due in part to temperature variations in the sample flowing through the densitometer which must remain isothermal if eq. (1) is to be strictly valid. Furthermore, compensation of density measurements for changes in the temperature of the sensor itself appeared to be faulty and therefore, a persistent problem in all experiments. Figure 12 is a comparison of the molecular weight estimates presented in Fig. 10 to actual molecular weight measurements obtained off-line from samples taken from the reactor during Experiment I. This figure shows significant differences between molecular weight measurements and on-line estimates which were essentially model predictions since no molecular weight measurements were available to update estimates.

Clearly, model accuracy must be improved to improve task level control performance. The kinetic parameters used in Experiment I are given in Table 3.

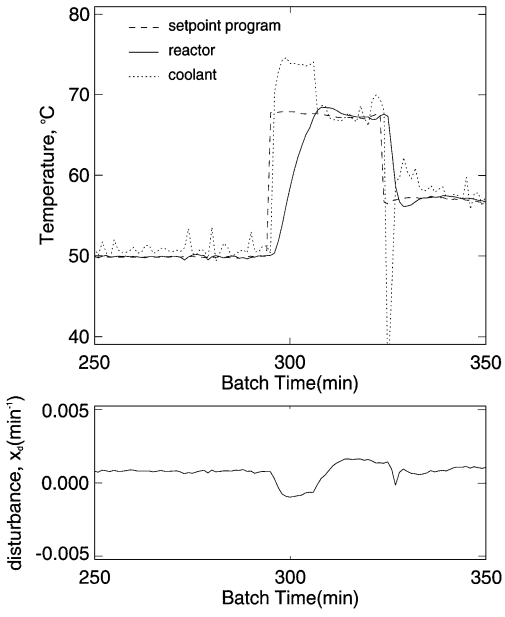

Fig. 9. Experiment I: Execution level temperature control.

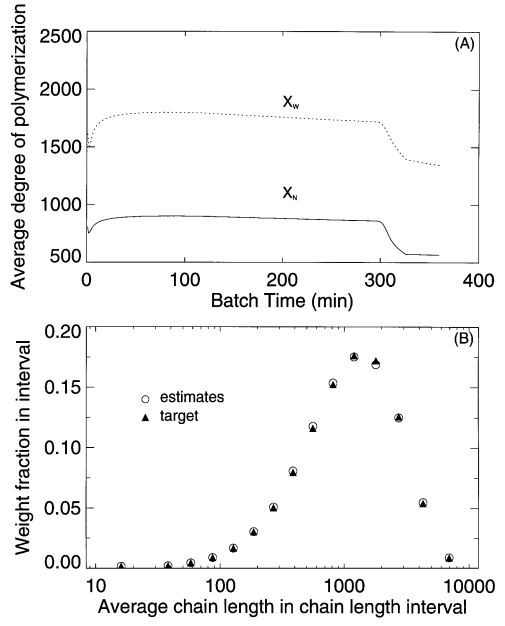

Fig. 10. Experiment I: calculated molecular weight averages and comparison of target and calculated WCLD at final conversion.

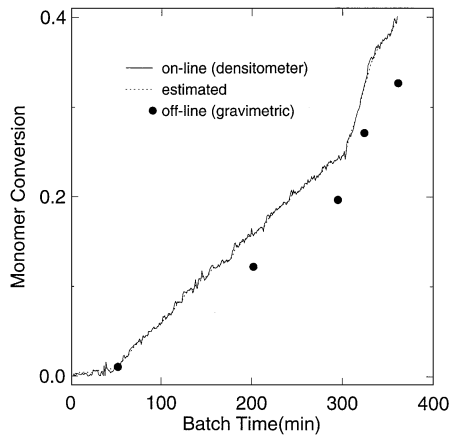

Fig. 11. Experiment I: comparison of on-line monomer conversion estimates and measurements to off-off-line measurements.

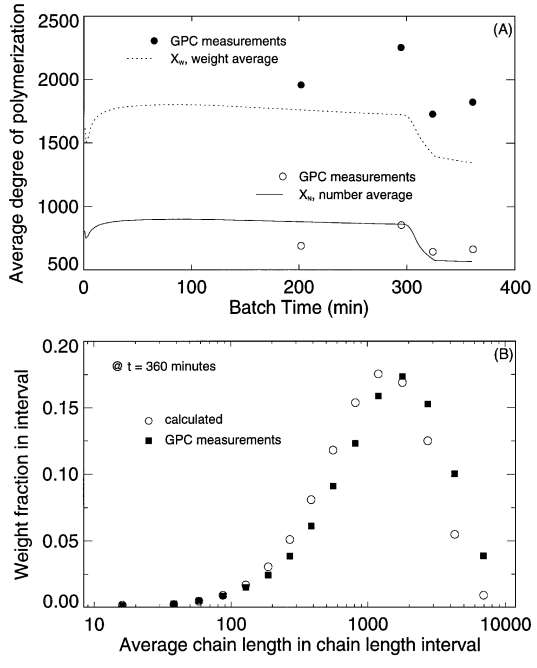

Fig. 12. Experiment I: comparison of calculated and measured molecular weight distributions and molecular weight averages.

Initiator efficiency factor, and monomer and solvent chain transfer frequency factors given in this table were obtained by fitting the model to experimental conversion and molecular weight distribution data for a batch polymerization under similar reaction conditions to those in Experiment I. All other kinetic parameter values were taken from the literature. The experimental polymerization used to find values for initiator efficiency factor and chain transfer frequency factors was an isothermal polymerization with only a very small amount of polymer produced under nonisothermal conditions at the end of the batch. Consequently, it was not feasible to obtain exact estimates of chain transfer activation energies and only the frequency factors were adjusted. Therefore, to improve model predictions, initiator efficiency factor and monomer chain transfer frequency factor and activation energy were reestimated using the experimental data from Experiment I which was clearly a nonisothermal experiment. For the refinement of these parameters, FSQP was used to minimize the

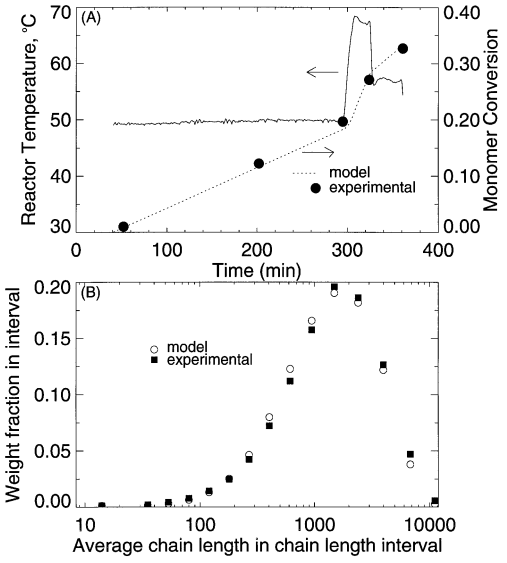

Fig. 13. Experiment I: model calculations with updated chain transfer constant and initiator efficiency factor.

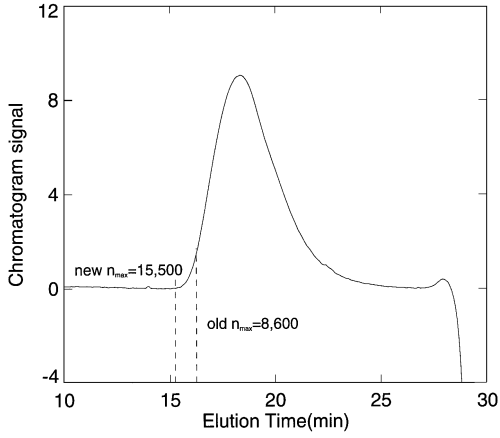

Fig. 14. Adjustment of maximum chain length to span the entire GPC chromatogram.

difference between the experimentally measured and model-predicted monomer conversion and MWD weight fractions. The results of this parameter optimization calculations are shown in Fig. 13. This figure shows that predictions of monomer conversion and the molecular weight distribution at final conversion now agree well with measurements of samples taken during Experiment I. Values for the reoptimized parameters, which are used in Experiments II and III, are given in Table 3.

Another problem encountered in Experiment I is illustrated in Fig. 14. This figure (GPC chromatogram) shows that the maximum chain length chosen to bound molecular weight distribution modeling (8600) corresponds to an elution time that does not span the full polymer chromatogram signal for a polymer sample taken at the end of Experiment I. Therefore, for Experiments II and III, the maximum chain length for modeling was increased to 15,500 to encompass the expected polymer chromatogram signals. Also, the target molecular weight distribution was set to the experimentally measured distribution at final conversion from Experiment I shown in Fig. 14 and given in Table 6. This represents a distribution with a weight average molecular weight of 182,000 and polydispersity of 2.75. To reduce the systematic error of densitometer measurements, sample flow rate through the densitometer was reduced in order to reduce the temperature rise caused by the relatively hot sample pumped from the reactor to the densitometer.

6.2. *State estimation*

Experiment II was conducted to verify that with a reasonably accurate process model, execution of the setpoint program will lead to the target molecular weight distribution and to demonstrate how estimates of molecular weight distribution can be improved using delayed MWD measurements. Because our experimental system is not equipped to make on-line molecular weight measurements, a molecular weight measurement from Experiment I was used as an approximate on-line measurement in Experiment II. The measurement was from a sample taken from the reactor during Experiment I at 295 min batch time. Monomer conversion for this sample was 20% as shown in Fig. 13(A). Also shown in this figure is that this sample represents polymer produced at a near constant temperature of 50°C. Therefore, to make the molecular weight distribution measurement from Experiment I a reasonable approximation, Experiment II was initially conducted under isothermal conditions at 50°C to about 24% conversion followed by an update of the molecular weight estimates using the approximate measurement and extended Kalman filter (EKF), after an assumed delay of 30 min. A suitable setpoint program is obtained by fixing the first three discrete temperature setpoints at 50°C, covering a monomer conversion range of 0 to 24% and computing the two remaining discrete temperature setpoint sequence which best matches the target molecular weight distribution at 40% conversion at the end of batch. Constraining the first three stages of the setpoint program was done because the unconstrained computed setpoint program, which is given in Fig. 20, is not isothermal during the first three discrete temperature setpoints.

Figure 15 presents the resulting suboptimal constrained temperature setpoint program represented by the final two discrete temperature setpoints covering monomer conversions from 24 to 40% corresponding to batch times of 234 min to 291 min. Again, the temperature setpoint is tracked reasonably well. The extended Kalman filter estimates of molecular weight averages and molecular weight distribution for Experiment II are shown in Fig. 16. Figure 16(A) shows that the EKF updates estimates of the three leading moments of the molecular weight distribution

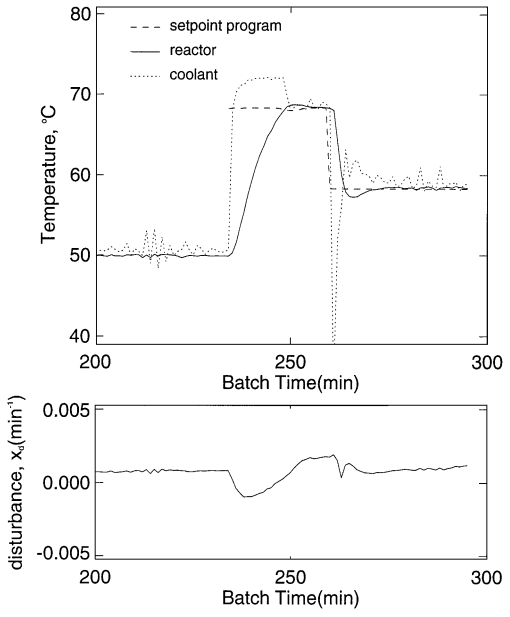

Fig. 15. Experiment II: execution level temperature control.

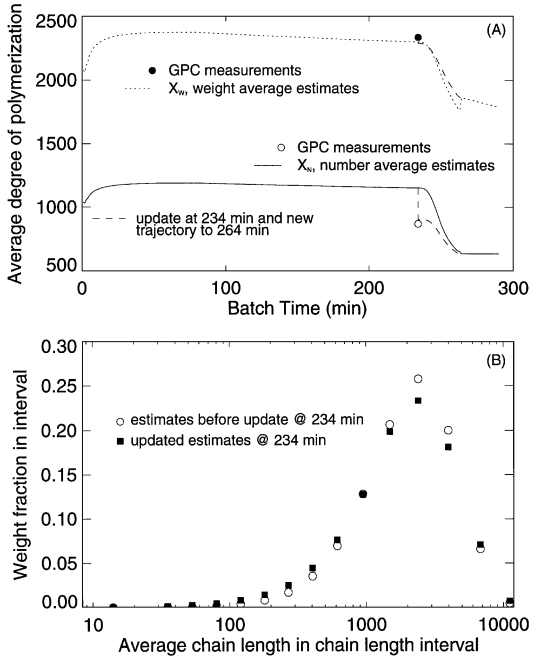

Fig. 16. Experiment II: on-line update of WCLD at 234 min batch time using measurement from Experiment I with 30 min measurement delay assumed.

using the approximate measurements of weight average and number average molecular weights from Experiment I as well as the current on-line measurement of monomer conversion in Experiment II which is essentially equivalent to a measurement of the first moment. The number and weight average degrees of polymerization shown in Fig. 16(A) are then calculated using the moment ratios given in eqs (27)–(28). The approximate measurement is assumed to have been made at a batch time of 234 min. Because the measurement delay is assumed to be 30 min, changes in the estimates reflecting the measurement are not seen until a batch time of 264 min as indicated by the small step changes in Fig. 16(A) at 264 min. Figure 16(B) presents on-line filter estimates of the molecular weight distribution at 24% conversion (234 min batch time) before and after updating with the delayed measurement. As seen in this figure, significant corrections to the estimate are made and specifically, the updated distribution has a higher polydispersity. This can be seen more clearly in Fig. 16(A) where at 264 min, the weight average molecular weight increases and the number average molecular weight decreases slightly, and therefore, the polydispersity ratio(X_w/X_n) increases from 2.0 to 2.53. In fact, measured polydispersity was consistently higher than corresponding model predictions for experimental samples analyzed, underscoring the importance of incorporating measurements to improve the accuracy of estimates.

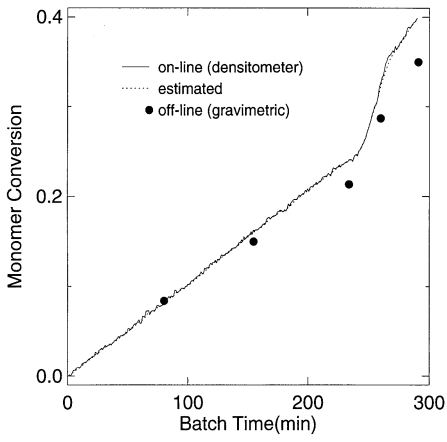

Fig. 17. Experiment II: comparison of on-line monomer conversion estimates and measurements to off-line measurements.

Once again, the real test of this method involves a comparison of on-line estimates to off-line measurements. During this experiment, five samples were taken at various batch times and monomer conversion and molecular weight distribution were measured off-line. Figure 17 shows that conversion measurements by densitometer are still slightly higher than the off-line gravimetric measurements, though the offset is signficantly less than in Experiment I. Also, because of a relatively low value specified for the measurement error covariance for polymer weight fraction (i.e. monomer conversion) and a relatively high value specified for the model error covariance of polymer weight fraction, the computed filter error covariances (filter gains) are large. This causes the filter to rely heavily on densitometer measurements to compute estimates of monomer conversion and the

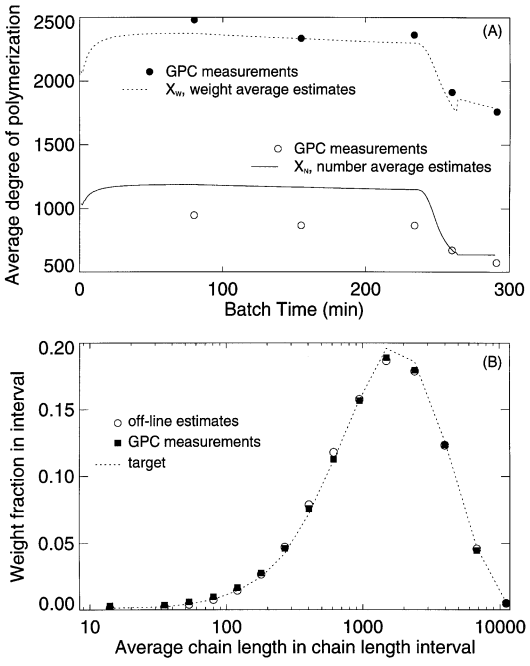

Fig. 18. Experiment II: comparison of on-line molecular weight averages and WCLD estimates at final conversion to off-line GPC measurements.

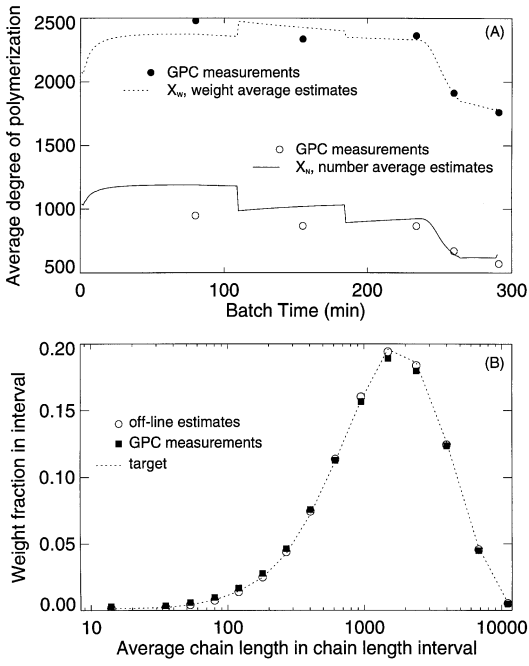

Fig. 19. Experiment II: estimation of molecular weight averages and WCLD with off-line GPC measurements with 30 min measurement delay (simulation).

result shown in Fig. 17 is that estimates track the measurement very closely.

Figure 18 shows that with a reasonably accurate process model and setpoint program design, the measured molecular weight distribution at final conversion (fifth sample) agrees well with the target chain length distribution and with on-line estimates of the distribution. Here, in Fig. 18(B), a line is drawn through the discrete target points for illustration purposes and not to indicate that the values presented are continuous. Furthermore, it is seen that with infrequent delayed molecular weight measurements (in this case we used one measurement from the previous experiment), estimation accuracy can be improved. If a system is equipped with on-line GPC equipment, given a long enough batch time it may be possible to incorporate molecular weight measurements taken at several times during the batch for estimation and control purposes. The simulation results shown in Fig. 19(A) illustrates such a possibility. Here, the five measurements taken in Experiment II are used to update estimates of the molecular weight averages and distribution for Experiment II in an off-line simulation, again assuming a 30 min measurement delay.

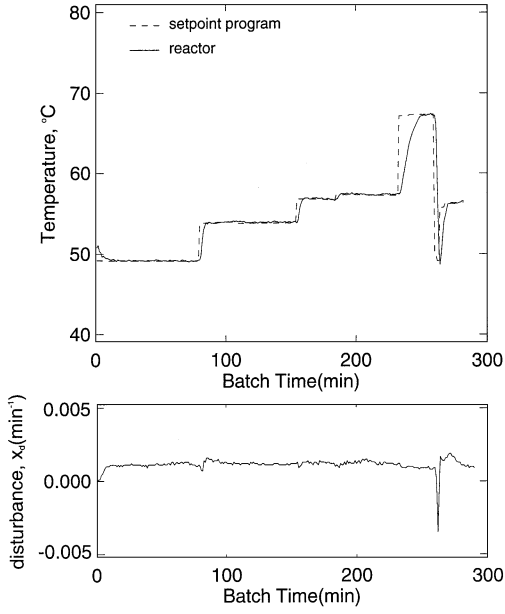

Fig. 20. Experiment III: execution level temperature control.

6.3. *Adjustment of temperature setpoint porogram*

In a real polymerization process, unknown process disturbances may lead to significant variations in polymer properties from target values. Therefore, it will be necessary to adjust the reactor conditions to correct these variations. A temperature setpoint program can be recomputed at each sampling time because the computation time required is relatively small. If updated estimates of molecular weight distribution using actual measurements causes significant discrepancies between the target and predicted distribution at final conversion based on the current setpoint program, then the optimizer (FSQP) will

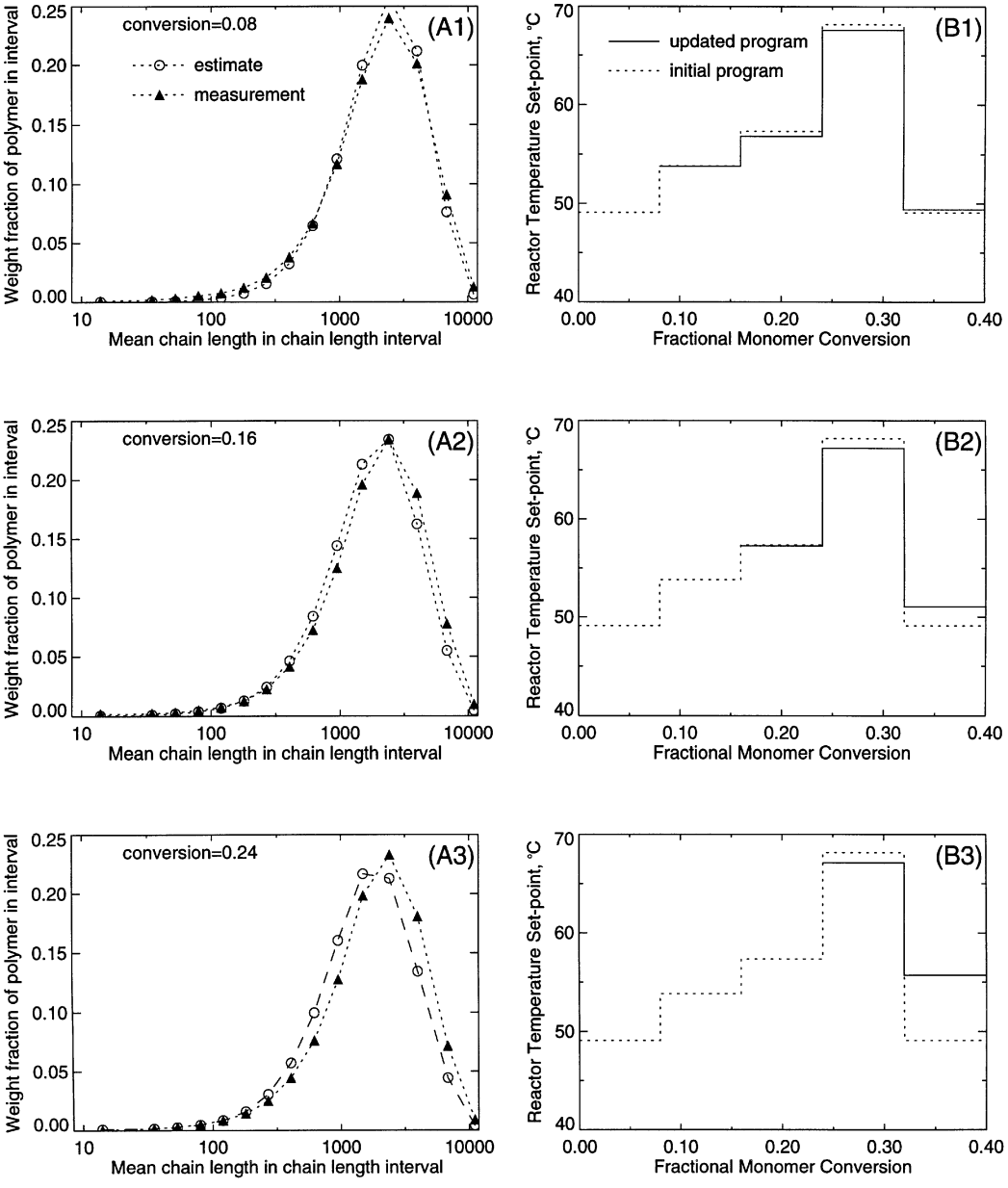

Fig. 21. On-line adjustment of temperature setpoint program.

recompute the setpoint program in the remaining batch period to minimize predicted discrepancies at final conversion. Experiment III was conducted to better illustrate how the task level control algorithm can adjust the setpoint program on-line when molecular weight measurements are used.

Experiment III was performed without polymerization but instead, using the on-line density measurements and off-line molecular weight measurements from Experiment II as mock measurements. The reactor itself was filled with solvent and actual temperatures of reactor (pure solvent), jacket and inlet coolant were used for tracking the computed setpoint program and for state estimation along with the mock measurements derived from Experiment II. Here, we remove the constraint that the first three stages of the setpoint program be fixed at 50°C, which was imposed only in Experiment II. Figure 20 presents the computed setpoint program and execution control during Experiment III. As seen in this figure, temperature profiles in Experiment III do not exactly match those in Experiment II. Therefore, we regard the use of experimental molecular weight and conversion measurements from Experiment II as a means of simulating realistic measurement error which may be encountered in an actual process. Figure 21 presents on-line estimates of molecular weight distribution before updating and the corresponding mock

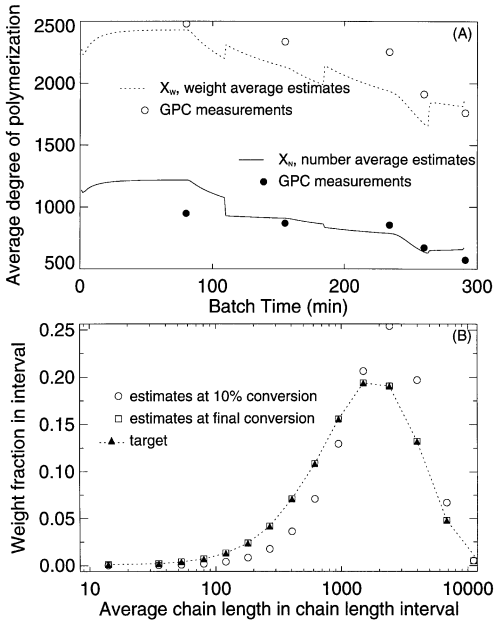

Fig. 22. Experiment III: on-line molecular weight estimates using delayed GPC measurements from Experiment II.

measurement for the first three samples taken from Experiment II. Figures on the right-hand side represent changes in the computed setpoint program which occurred as a result of updating the molecular weight distribution estimates. Finally, Fig. 22 shows that these setpoint program adjustments drive the on-line estimated molecular weight distribution to the target distribution at final conversion. Also shown in Fig. 22(B) is the weight chain length distribution at 10% conversion for comparison.

Since this was not an actual polymerization experiment, we cannot make the crucial comparison of measured molecular weight distribution to the target. Nevertheless, this result clearly illustrates that with some on-line measurements of polymer MWD, it is possible to adjust the reactor temperature on-line and obtain the desired final MWD.

7. CONCLUDING REMARKS

Traditionally, molecular weight averages and polydispersity have been used as a measure of polymer molecular weight distribution and controlled in industrial polymerization processes. In this paper, we have presented a novel on-line MWD control technique to produce polymers with a target WCLD in a batch free radical polymerization process. This strategy uses a detailed polymerization process model and decoupled extended Kalman filters to estimate state variables and polymer molecular weight using rapid on-line measurements of temperature and monomer conversion together with less frequent and time delayed GPC measurements of WCLD. For the design of MWD control system, a task level controller is first designed to determine the reactor temperature set point profiles that will lead to a desired monomer conversion and MWD at the end of batch operation. For the calculation of polymer chain length distribution, the method of finite molecular weight moments was used. At each sampling time, a task level controller finds the best values for a sequence of reactor temperature setpoints using an optimization program based on sequential quadratic programming. Then, the temperature setpoint program is adjusted on-line. The same optimization program is also used by an execution level temperature controller to compute values for jacket feed temperature which best track the set points computed by the task level controller. To test the feasibility of the proposed MWD control technique, laboratory control experiments have been carried out for solution polymerization of methyl methacrylate. Our simulation and experimental results suggest that the proposed control strategy can be an useful new technique to control the WCLD of polymer in a batch free radical polymerization process.

Acknowledgment

This work was supported in part by the sponsors of the Chemical Process Systems Laboratory, a constituent laboratory of the Institute for Systems Research, and by LG Chemical Company. Insightful comments by an anonymous reviewer are also appreciated.

NOTATION

c_p	heat capacity of reaction mixture, cal $g^{-1} K^{-1}$
c_{pc}	heat capacity of coolant, cal $g^{-1} K^{-1}$
D_n	dead polymer concentration with n repeating units, mol L^{-1}
$f(m, n)$	weight fraction of polymer in chain length interval from m, n
$f_{i,\mathrm{set}}$	target weight fraction for ith fraction of WCLD
f_i	initiator efficiency factor
g_t	gel effect parameter
$(-\Delta H)$	heat of polymerization, cal mol^{-1}
I	initiator concentration, mol L^{-1}
I_0	initial initiator concentration, mol L^{-1}
$J(\underline{u}, x_{cf})$	objective function for weight chain length distribution control
$J_k(\underline{u}_k, x_{cf})$	value of objective function at kth sampling time
J'_k	objective function for reactor temperature control
k_d	initiator decomposition rate constant, min^{-1}
k_{fm}	chain transfer to monomer rate constant, L $mol^{-1} min^{-1}$
k_{fs}	chain transfer to solvent rate constant, L $mol^{-1} min^{-1}$
k_i	primary radical formation rate constant, L $mol^{-1} min^{-1}$
k_p	propagation rate constant, L $mol^{-1} min^{-1}$

k_{td} disproportionation termination rate constant, L mol^{-1} min^{-1}
M monomer concentration, mol L^{-1}
M_t total reaction mass, g
M_n dead polymer concentration with n repeating units, mol L^{-1}
$\bar{M}_n$ number average molecular weight, g mol^{-1}
$\bar{M}_w$ weight-average molecular weight, g mol^{-1}
M_0 initial monomer concentration, mol L^{-1}
N number of optimized future moves for manipulated variable T_c
p prediction horizon for temperature controller
P total concentration of live polymer radicals, mol L^{-1}
P_n live polymer radical concentration with n repeating units, mol L^{-1}
q_c coolant flow rate, L min^{-1}
q_r jacket recycle flow rate parameter, L min^{-1}
R primary radical concentration, mol L^{-1}
S solvent concentration, mol L^{-1}
u_c dimensionless coolant feed temperature
$u_{c,k}$ coolant feed temperature at kth sampling time, K
v_1 volume of jacket section 1, L
v_2 volume of jacket section 2, L
v_f free volume
$v_{f,cr}$ critical free volume
$\mathbf{u}$ vector of optimized reactor temperature setpoints
$\mathbf{u}_k$ vector of optimized reactor temperature setpoints at kth sampling time
$\mathbf{u}_0$ initial values for sequence of reactor temperature setpoints
u_j jth element of vector u
$u_{j,k}$ jth element of vector u_k
u_{eff} effective heat transfer coefficient, cal K^{-1} min^{-1}
V reactor volume, L
V_J jacket volume, L
w_m monomer molecular weight, g mol^{-1}
x_c monomer conversion
x_{cf} final monomer conversion
x_d disturbance state
x_j weight fraction of component j
x_J dimensionless jacket temperature
x_{m0} initial monomer weight fraction
x_T dimensionless reactor temperature

Greek letters

α probability of propagation
λ_k^l kth moment of live polymer molecular weight distribution
λ_k kth moment of dead polymer molecular weight distribution
ρ_j density of component j
ϕ_m monomer volume fraction
ϕ_{m0} initial monomer volume fraction
ϕ_s solvent volume fraction
ϕ_{s0} initial solvent volume fraction
ϕ_p polymer volume fraction

REFERENCES

Adebekun, D. K. and Schork, F. J. (1989) Continuous solution polymerization reactor control. 2. Estimation and nonlinear reference control during methyl methacrylate polymerization. *Ind. Engng Chem. Res.* **28**, 1846–1861.

Bazaraa, M. S., Sherali, H. D. and Shetty, C. M. (1993) *Nonlinear Programming, Theory and Algorithms.* Wiley, New York.

Bersted, B. H. and Anderson, T. G. (1990) Influence of molecular weight and molecular weight distribution on the tensile properties of amorphous polymers. *J. Appl. Polym. Sci.* **39**, 499–514.

Beste, L. F. and Hall, jr., H. K. (1966) Equations for continuous control of molecular weight distribution in homogeneous free-radical polymerizations. *J. Macromol. Chem.* **1**, 121–135.

Choi, K. Y. and Butala, D. N. (1991) An experimental study of multiobjective dynamic optimization of a semibatch copolymerization process. *Polym. Engng Sci.* **31**(5), 353–364.

Crowley, T. J. and Choi, K. Y. (1997a) Calculation of molecular weight distribution from molecular weight moments in free radical polymerization. *Ind. Engng Chem. Res.* **36**, 1419–1423.

Crowley, T. J. and Choi, K. Y. (1997b) Discrete optimal control of molecular weight distribution in batch free radical process. *Ind. Engng Chem. Res.* **36**(9), 3676–3684.

Cuthrell, J. E. and Biegler, L. T. (1989) Simulataneous optimization and solution methods for batch reactor control profiles. *Comput. Chem. Engng* **13**(12), 49–62.

DuPont Company Product Bulletin. *VAZO Polymerization Initiators.*

Ellis, E. F., Taylor, T. W. and Jensen, K. F. (1988) Estimation of the molecular weight distribution in batch polymerization. *A.I.Ch.E.J.* **34**(8), 1341–1352.

Ellis, E. F., Taylor, T. W. and Jensen, K. F. (1994) On-line estimation molecular weight distribution estimation and control in batch polymerization. *A.I.Ch.E.J.* **40**(3), 445–462.

Garcia, C. E. and Morshedi, A. M. (1986) Quadratic programming solution of dynamic matrix control(QDMC). *Chem. Engng Commun.* **46**, 73–87.

Hicks, G. A. and Ray, W. H. (1971) Approximation methods for optimal control synthesis. *Can. J. Chem. Engng* **49**, 522–528.

Hoffman, R. F., Schreiber, S. and Rosen, G. (1964) Batch polymerization: narrowing molecular weight distribution. *Ind. Engng Chem.* **56**(5), 51–57.

Kim, K. J. and Choi, K. Y. (1991) On-line estimation and control of a continuous stirred tank polymerization reactor. *J. Proc. Cont.* **1**, 96–109.

Kozub, D. J. and MacGregor, J. F. (1992) Feedback control of polymer quality in semi-batch copolymerization reactors. *Chem. Engng Sci.* **47**(4), 929–942.

Maschio, G., Bello, T. and Scali, C. (1994) Optimal operation strategies to control the molecular weight of polymer products. *Chem. Engng Sci.* **49**(24B), 5071–5086.

Ogunnaike, B. A. (1994) On-line modelling and predictive control of an industrial terpolymerization reactor. *Int. J. Control* **59** (3), 711–729.

Panier, E. R. and Tits, A. L. (1993) On combining feasibility, descent and superlinear convergence in inequality contrained optimization. *Math. Programming*, **59**, 261–276.

Ponnuswamy, S. R., Shah, S. L. and Kiparissides, C. A. (1987) Computer optimal control of batch polymerization reactors. *Ind. Engng Chem. Res.* **26,** 2229–2236.

Ray, W. H. (1972) On the mathematical modeling of polymerization reactors. *J. Macromol. Sci.- Revs. Macromol. Chem.* **C8**(1), 1–56.

Ray, W. H. (1986) Polymerization reactor control. *IEEE Control Systems Mag.* **8**, 3–8.

Ross, R. T. and Laurence, R. L. (1976) Gel effect and free volume in the bulk polymerization of methyl methacrylate. *A.I.Ch.E. Symp. Ser.* **72**, 74–79.

Sacks, M. E., Lee, S. I. and Biesenberger, J. A. (1973) Effect of temperature variations on molecular weight distributions: batch, chain addition polymerizations. *Chem. Engng Sci.* **28**(1–P), 241–257.

Schmidt, A. D. and Ray, W. H. (1981) The dynamic behavior of continuous polymerization reactors-I, isothermal solution polymerization in a CSTR. *Chem. Engng Sci.* **36,** 1401–1410.

Schuler, H. and Suzhen, Z. (1985) Real time estimation of the chain length distribution in a polymerization reactor. *Chem. Engng Sci.* **40**(10), 1891–1904.

Tabak, D. and Kuo, B. C. (1969) Application of mathematical programming in the design of optimal control systems. *Int. J. Control* **10**(5), 545–552.

Thomas, I. M. and Kiparissides, C. (1984) Computation of the near-optimal temperature and initiator policies for a batch polymerization reactor. *Can. J. Chem. Engng* **62**, 284–291.

Tirrell, M. and Gromley, K. (1981) Composition control of batch copolymerization reactors. *Chem. Engng Sci.* **36**(2-I), 367–375.